# FORCE-UNCONSTRAINED POSES OF THE 3-PRR AND 4-PRR PLANAR PARALLEL MANIPULATORS

**Flavio Firmani and Ron P. Podhorodeski**†
Robotics and Mechanisms Laboratory, Department of Mechanical Engineering,
University of Victoria, P. O. Box 3055, Victoria, B. C., Canada,V8W 3P6
{ffirmani, podhoro}@me.uvic.ca
†Corresponding author: Fax: (250)-721-6051

## Abstract

Force-unconstrained (singular) poses of the 3-PRR planar parallel manipulator (PPM), where the underscore indicates the actuated joint, and the 4-PRR, a redundant PPM with an additional actuated branch, are presented. The solution of these problems is based upon concepts of reciprocal screw quantities and kinematic analysis. In general, non-redundant PPMs such as the 3-PRR are known to have two orders of infinity of force-unconstrained poses, i.e., a three-variable polynomial in terms of the task-space variables (position and orientation of the mobile platform). The inclusion of redundant branches eliminates one order of infinity of force-unconstrained configurations for every actuated branch beyond three. The geometric identification of force-unconstrained poses is carried out by assuming one variable for each order of infinity. In order to simplify the algebraic procedure of these problems, the assumed or "free" variables are considered to be joint displacements. For both manipulators, an effective elimination technique is adopted. For the 3-PRR, the roots of a $6^{th}$-order polynomial determine the force-unconstrained poses, i.e., surfaces in a three dimensional space defined by the task-space variables. For the 4-PRR, a $64^{th}$-order polynomial determines curves of force-unconstrained poses in the same dimensional space.

# Poses singulières des manipulateurs parallèles plans 3-PRR et 4-PRR

## Résumé

Les poses singulières des Manipulateurs Parallèles Plans (MPP) 3-PRR, où la lettre soulignée indique le joint actionné, et 4-PRR, un MPP à actionnement redondant, sont présentées. La solution de ces problèmes est basée sur les concepts de visseurs réciproques et d'analyse cinématique. En général, les MPP non redondants tels que le 3-PRR sont connus pour avoir deux ordres d'infinité de poses singulières, i.e., un polynôme dont les trois variables sont la position et l'orientation de la plate-forme mobile. L'inclusion de chaînes redondantes élimine un ordre d'infinité de poses singulières pour chaque chaîne actionnée au-delà de trois. L'identification géométrique des poses singulières est effectuée en considérant une variable par ordre d'infinité. Afin de simplifier la résolution de ce problème, les déplacements des articulations sont les variables considérées dans cet article. Pour les deux manipulateurs, une technique d'élimination efficace est adoptée. Pour le 3-PRR, les racines d'un polynôme de degré 6 déterminent les poses singulières qui forment des surfaces dans l'espace tridimensionnel défini par la position de l'orientation de la plate-forme mobile. Pour le 4-PRR, un polynôme de degré 64 détermine les poses singulières qui forment des courbes dans ce même espace tridimensionnel.

# 1 Introduction

Parallel manipulators (PMs) compared to serial manipulators have higher structural stiffness and greater payload accuracy but smaller and less dexterous workspaces. In addition, PMs can have force-degenerate configurations. Merlet [1] defined that a singular configuration of a PM corresponds to a configuration where it is not rigid, i.e., a force-degenerate configuration. If the branch resultant forces together do not span the system of forces to be applied or sustained, the manipulator is degenerate and is force unconstrained. Physically, the mobile platform can have motion even if all actuated joints are locked, i.e., the manipulator may instantaneously gain one or more unconstrained degrees of freedom (DOFs).

Gosselin and Angeles [2] analyzed singularities in Jacobian matrices resulting from differentiating the nonlinear kinematic constraints $f(\boldsymbol{\theta}, \mathbf{x})$ of the input and output variables, with respect to (wrt) time. This leads to a relationship, $[\mathbf{A}]\,\dot{\mathbf{x}} + [\mathbf{B}]\,\dot{\boldsymbol{\theta}} = \mathbf{0}$ of input and output speeds, where $[\mathbf{A}] = \partial f(\boldsymbol{\theta}, \mathbf{x})/\partial \mathbf{x}$ and $[\mathbf{B}] = \partial f(\boldsymbol{\theta}, \mathbf{x})/\partial \boldsymbol{\theta}$ are both $m \times m$ Jacobian matrices with $m$ being the number of DOFs of the linkage. Three different types of singularities were reported for closed kinematic chains: Type I (instantaneous motion singularity) occurs when $[\mathbf{B}]$ is singular, Type II (force singularity) occurs when $[\mathbf{A}]$ is singular, and Type III occurs when both are singular.

For planar manipulators, three dimensions of task-space coordinates exist. These coordinates can be represented by the location ($x$ and $y$) and orientation ($\phi$) of the mobile platform. Sefrioui and Gosselin [3] identified the singular poses of the 3-R$\underline{\text{P}}$R layout. For constant payload orientation, these singularities can be plotted as quadratic curves in the $xy$ plane. Bonev and Gosselin [4] reported that, for constant orientation, the singularity loci of all branch arrangements of the 3-$\underline{\text{R}}$RR configuration can be represented by curves of degree 42. Chan and Ebert-Uphoff [5] determined the manifold of singularities and showed how unconstrained motions are projected on it. Bonev [6] and Bonev, Zlatanov and Gosselin [7] presented a detailed study of the singular configurations of all possible actuation configurations of 3-DOF PPMs via screw theory.

For non-redundant PPMs, the number of actuators $n$ and DOF $m$ are equal. Merlet [8] described that the inclusion of redundant actuators may lead to improvements in various analyses such as forward kinematics, singular configurations, and optimal force control and calibration. In order to reduce uncertainty configurations, Notash and Podhorodeski considered over-constrained parallel manipulators by including either redundant actuation within branch(es) [9] or redundant branches [10]. Nokleby, Fisher, Podhorodeski, and Firmani [11] demonstrated that the use of redundant actuation within branches improves significantly the force capabilities of parallel manipulators. Collins [12] proposed a method for choosing redundant actuator locations that provide singularity-free motions. Pseudoinverse techniques were applied for solving the inverse of the Jacobian. Dasguspa and Mruthyunjaya [13] showed that the use of redundant actuation leads to a reduction or even an elimination of force singularities. Similarly, O'Brien and Wen [14] showed that the use of redundancy improves the manipulability of the original mechanism by comparing the condition number of non-redundant and redundant manipulators. Chan [15] considered that using a single redundant actuator the dimension of the manifold of singularities can be reduced by an order of one. Firmani and Podhorodeski [16] and [17] eliminated families of force unconstrained configurations by including redundant actuation within one branch. Furthermore, Firmani and Podhorodeski [18] investigated the force-unconstrained poses of the 4-R$\underline{\text{P}}$R manipulator by considering the force-unconstrained poses of two three-branch assemblies, then by means of Gröbner Bases determining a polynomial in terms of two task-space variables.

The outline of the remainder of the paper is as follows. In Section 2 and 3, the force-unconstrained poses of the 3-$\underline{\text{P}}$RR and 4-$\underline{\text{P}}$RR are presented. Section 4 is a discussion of the results. The paper finishes with conclusions in Section 5.

# 2 3-PRR Manipulator

## 2.1 Background

The 3-PRR manipulator was first introduced by Gosselin, Lemieux, and Merlet [19]. Each branch is composed of a prismatic joint fixed to the base, followed by two revolute joints separated by a link. In order to reduce the inertia of the mechanism, the prismatic joints are actuated allowing high speed applications. In [19], the kinematic analysis of the inverse and forward problems, the input and output speed Jacobian matrices, and a workspace description were presented.

For a constant payload orientation, Bonev [6] and Bonev, Zlatanov and Gosselin [7] identified the singular configurations of this manipulator. These configurations can be represented by a $20^{th}$-order multivariable polynomial in terms of $x$ and $y$. However, an exhaustive process of simplification, due to the fact that the resulting equation is expressed in terms of square roots, is required. The geometric identification of the singular poses requires $\phi$ to be varied, i.e., $0 \leqslant \phi < 2\pi$, making this method computationally expensive.

To the best of the authors' knowledge, no mathematical software can determine a single symbolic expression for force-unconstrained poses of the 3-PRR in terms of $x$, $y$, and $\phi$. Nevertheless, if a symbolic expression were to be found, the force-unconstrained poses could be plotted by assuming two of these variables, i.e., there is an order of two infinities $\left(O\left(\infty^2\right)\right)$ of choices. In order to make the solution more efficient the two"free" variables are chosen to be joint displacements.

In this section, the force-unconstrained poses of the 3-PRR are identified. First the Denavit and Hartenberg (D&H) parameters [20] of each branch are determined. Second, screws and associated reciprocal screws are found. Third, the loop-closure equations that define the geometry of the manipulator are derived. Fourth, the elimination process is carried out by properly selecting the "free" variables and the force-unconstrained poses are identified.

## 2.2 Denavit and Hartenberg Parameters

The notation of the geometric variables of the manipulator are shown in Figure 1. The homogeneous transform of each branch base $b_i$ wrt to *{0}* is shown below. D&H parameters describing the 3-PRR layout are given in Table 1, where $j$ and $i$ represent the joint and branch numbers, respectively, and *{ref}* is a reference frame located at $\{3_1\}$. To keep the D&H parameters in a general form $l_1 = 0$, $\beta_1 = 0$, $\beta_2 = \pi$, and $\beta_3 = \pi - \alpha_3$.

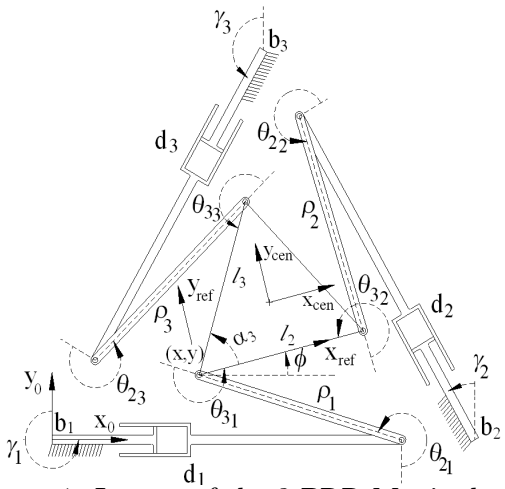


Figure 1: Layout of the 3-PRR Manipulator

$$\left[{}^{0}_{b_i}\mathbf{T}\right] = \begin{bmatrix} \cos(\gamma_i) & -\sin(\gamma_i) & 0 & bx_i \\ \sin(\gamma_i) & \cos(\gamma_i) & 0 & by_i \\ 0 & 0 & 1 & 0 \\ 0 & 0 & 0 & 1 \end{bmatrix}$$

| $j-1$ | $\alpha_{j-1}$ | $a_{j-1}$ | $d_j$ | $\theta_{j_i}$ | $j$ |
|---|---|---|---|---|---|
| $b_i$ | $-\frac{1}{2}\pi$ | 0 | $d_i$ | 0 | $1_i$ |
| $1_i$ | $\frac{1}{2}\pi$ | 0 | 0 | $\theta_{2_i}$ | $2_i$ |
| $2_i$ | 0 | $\rho_i$ | 0 | $\theta_{3_i}$ | $3_i$ |
| $3_i$ | 0 | $l_i$ | 0 | $\beta_i$ | $ref$ |

Table 1: DH Parameters of the 3-PRR

### 2.3 Screw Quantities

The identification of the singular poses is based upon screw quantities ( see [21], [22], [23], and [24], for further detail). The static force relationship is given by $\mathbf{F} = [\mathbf{W}]\,\mathbf{w}$, where $\mathbf{F}$ is the generalized applied force (wrench), $\mathbf{w} = \begin{bmatrix} w_1 & w_2 & w_3 \end{bmatrix}^{\mathrm{T}}$ is the vector of wrench intensities, and $[\mathbf{W}]$ is the associated reciprocal screw (ARS) matrix. As shown in [18] the ARS matrix is equivalent to the combined Jacobian $[\mathbf{W}] \equiv [\mathbf{J}]^{\mathrm{T}}$, where $[\mathbf{J}] = [\mathbf{B}]^{-1}[\mathbf{A}]$. If the applied force is given and the vector of intensities is unknown, inversion of $[\mathbf{W}]$ allows $\mathbf{w}$ to be found; however, if $[\mathbf{W}]$ is singular, an arbitrary force $\mathbf{F}$ cannot be sustained, i.e., the device is force unconstrained.

Resolving $[\mathbf{W}]$ requires finding the screw coordinates of all joints of each branch wrt *{ref}*. Manipulator joints can be modeled with their screw coordinates as follows [25]:

$$ {}^{\mathrm{ref}}\$_{j_i} = \left\{ {}^{\mathrm{ref}}\vec{\mathbf{z}}_{j_i}^{\mathrm{T}};\ \left( {}^{(\mathrm{ref}}\vec{\mathbf{r}}_{\mathrm{ref}\rightarrow j_i} \times {}^{\mathrm{ref}}\vec{\mathbf{z}}_{j_i} + p_{_L}\, {}^{\mathrm{ref}}\vec{\mathbf{z}}_{j_i} \right)^{\mathrm{T}} \right\}^{\mathrm{T}} \tag{1} $$

where $p_{_L}$ is the associated pitch ($p_{_L} = 0$ for revolute, and $p_{_L} = \infty$ for prismatic, joints), and ${}^{\mathrm{ref}}\vec{\mathbf{z}}_{j_i}$ and $( {}^{\mathrm{ref}}\vec{\mathbf{r}}_{\mathrm{ref}\rightarrow j_i} \times {}^{\mathrm{ref}}\vec{\mathbf{z}}_{j_i})$ are the direction and moment of the $j^{th}$ joint of the $i^{th}$ branch wrt *{ref}*, respectively. For the 3-PRR , the following joint screws[1] written in matrix form per branch result:

$$ {}^{\mathrm{ref}}[\$_1] = \begin{bmatrix} {}^{\mathrm{ref}}\$_{1_1} & {}^{\mathrm{ref}}\$_{2_1} & {}^{\mathrm{ref}}\$_{3_1} \end{bmatrix} = \begin{bmatrix} 0 & 1 & 1 \\ \sin(\theta_{2_1}+\theta_{3_1}) & \rho_1 \sin(\theta_{3_1}) & 0 \\ \cos(\theta_{2_1}+\theta_{3_1}) & \rho_1 \cos(\theta_{3_1}) & 0 \end{bmatrix} $$

$$ {}^{\mathrm{ref}}[\$_2] = \begin{bmatrix} {}^{\mathrm{ref}}\$_{1_2} & {}^{\mathrm{ref}}\$_{2_2} & {}^{\mathrm{ref}}\$_{3_2} \end{bmatrix} = \begin{bmatrix} 0 & 1 & 1 \\ -\sin(\theta_{2_2}+\theta_{3_2}) & -\rho_2 \sin\theta_{3_2} & 0 \\ -\cos(\theta_{2_2}+\theta_{3_2}) & -\rho_2 \cos\theta_{3_2} - l_2 & -l_2 \end{bmatrix} $$

$$ {}^{\mathrm{ref}}[\$_3] = \begin{bmatrix} {}^{\mathrm{ref}}\$_{1_3} & {}^{\mathrm{ref}}\$_{2_3} & {}^{\mathrm{ref}}\$_{3_3} \end{bmatrix} = \begin{bmatrix} 0 & 1 & 1 \\ -\sin(\theta_{2_3}+\theta_{3_3}-\alpha_3) & -\rho_3 \sin(\theta_{3_3}-\alpha_3) + l_3 \sin\alpha_3 & l_3 \sin\alpha_3 \\ -\cos(\theta_{2_3}+\theta_{3_3}-\alpha_3) & -\rho_3 \cos(\theta_{3_3}-\alpha_3) - l_3 \cos\alpha_3 & -l_3 \cos\alpha_3 \end{bmatrix} $$

The ARS of an actuated joint of a branch is reciprocal to all other joints in the branch except for the actuated joint. Mathematically, two screws $\mathbf{A} = \{\mathbf{a}^{\mathrm{T}}; \mathbf{a}_o^{\mathrm{T}}\}^{\mathrm{T}}$ and $\mathbf{B} = \{\mathbf{b}^{\mathrm{T}}; \mathbf{b}_o^{\mathrm{T}}\}^{\mathrm{T}}$ are reciprocal if their reciprocal product is zero, i.e., $\mathbf{A} \circledast \mathbf{B} = \mathbf{a} \cdot \mathbf{b}_o + \mathbf{a}_o \cdot \mathbf{b} = 0$. The prismatic joint of each branch is actuated, i.e., $W_{1_i} \circledast \$_{j_i} = 0$ for j $\neq$1. The reciprocal screws are then used to assemble the ARS matrix. Notice that when $w_i > 0$ the $i^{th}$ branch pushes the mobile platform, for $i = 1, 2, 3$.

$$ {}^{\mathrm{ref}}[\mathbf{W}] = \begin{bmatrix} {}^{\mathrm{ref}}W_{1_1} & {}^{\mathrm{ref}}W_{1_2} & {}^{\mathrm{ref}}W_{1_3} \end{bmatrix} = \begin{bmatrix} \cos\theta_{3_1} & -\cos\theta_{3_2} & -\cos(\theta_{3_3}-\alpha_3) \\ -\sin\theta_{3_1} & \sin\theta_{3_2} & \sin(\theta_{3_3}-\alpha_3) \\ 0 & l_2 \sin\theta_{3_2} & l_3 \sin\theta_{3_3} \end{bmatrix} \tag{2} $$

As mentioned before, if ${}^{\mathrm{ref}}[\mathbf{W}]$ becomes singular an arbitrary force $\mathbf{F}$ cannot be sustained. This occurs when its determinant is equal to zero, i.e.,

$$ \begin{aligned} \left| {}^{\mathrm{ref}}[\mathbf{W}] \right| &= l_2 \sin(\theta_{3_2}) \left( \sin(\theta_{3_1}) \cos(\theta_{3_3}-\alpha_3) - \cos(\theta_{3_1}) \sin(\theta_{3_3}-\alpha_3) \right) \\ &\quad + l_3 \sin(\theta_{3_3}) \left( \cos(\theta_{3_1}) \sin(\theta_{3_2}) - \sin(\theta_{3_1}) \cos(\theta_{3_2}) \right) = 0 \end{aligned} \tag{3} $$

### 2.4 Loop-Closure Equations

The relationship between the joint angles of the $i^{th}$ branch and the pose ($x$, $y$ and $\phi$) of the mobile platform is defined by the loop-closure equation that describe *{ref}* wrt *{0}*, i.e.,

$$ \begin{aligned} x &= bx_i - d_i \sin(\gamma_i) + \rho_i \cos(\gamma_i + \theta_{2_i}) + l_i \cos(\gamma_i + \theta_{2_i} + \theta_{3_i}) \\ y &= by_i + d_i \cos(\gamma_i) + \rho_i \sin(\gamma_i + \theta_{2_i}) + l_i \sin(\gamma_i + \theta_{2_i} + \theta_{3_i}) \\ \phi &= \gamma_i + \theta_{2_i} + \theta_{3_i} + \beta_i \end{aligned} \tag{4} $$

[1] For the planar case $\$_{j_i} = \{L,\ M,\ N;\ P,\ Q,\ R\}^{\mathrm{T}} = \{0,\ 0,\ N;\ P,\ Q,\ 0\}^{\mathrm{T}}$, therefore, for simplification, the zero elements of $\$_{j_i}$ ($L$, $M$, and $R$) do not need to be shown.

In order to eliminate $\theta_{2_i}$ and $d_i$, Eqs. (4) are sequentially substituted, yielding

$$\begin{aligned} f_i(x,\ y,\ \phi,\ \theta_{3_i}) &= (y - by_i - \rho_i \sin(\phi - \theta_{3_i} - \beta_i) - l_i \sin(\phi - \beta_i)) \sin(\gamma_i) \\ &\quad + (x - bx_i - \rho_i \cos(\phi - \theta_{3_i} - \beta_i) - l_i \cos(\phi - \beta_i)) \cos(\gamma_i) = 0 \end{aligned} \tag{5}$$

### 2.5 Force-Unconstrained Poses

There are four equations (Eq.(3) and Eqs. (5), $i = 1, 2, 3$) and six variables ($x$, $y$, $\phi$, and $\theta_{3_i}$, for $i = 1, 2, 3$). It would be desirable to eliminate all $\theta_{3_i}$ and remain with an expression in terms of the task space variables; however, this elimination cannot be performed symbolically, because there are nonlinear terms (square roots), and their elimination requires squaring already large equations.

A more efficient way to solve this problem is to choose the "free" variables to be two of the third joint angles, for example $\theta_{3_1}$ and $\theta_{3_2}$. This allows us to compute $\theta_{3_3}$ from Eq. (3), yielding two possible solutions, $\theta_{3_3}$ and $\theta_{3_3} - \pi$. Both $\theta_{3_3}$ solutions make the third ARS intersect the common point of the other two ARSs. The $\theta_{3_i}$ values define the orientation of links $\rho_i$ wrt the platform.

Now the problem is reduced to assembling the links with the arrangement of the prismatic joints using the loop-closure equations. The numerical values of $\theta_{3_i}$ are substituted in Eq. (5). Half-angle substitution[2] is applied to $\phi$ and the loop-closure equations Eq. (5) become a function of $x$, $y$, and $t$, the last being a quadratic variable. These equations are written in matrix form as

$$[\Psi]\ \mathbf{x} = \begin{bmatrix} \psi_{11} & \psi_{12} & \psi_{13} \\ \psi_{21} & \psi_{22} & \psi_{23} \\ \psi_{31} & \psi_{32} & \psi_{33} \end{bmatrix} \begin{bmatrix} x \\ y \\ 1 \end{bmatrix} = \mathbf{0} \tag{6}$$

where the elements of $[\Psi]$ are quadratic polynomials in $t$ and constants and $\mathbf{0}$ is a 3 by 1 null vector.

In order to satisfy Eq. (6), matrix $[\Psi]$ has to be singular, i.e., $|[\Psi]| = 0$. Since each element of $[\Psi]$ is a quadratic polynomial in $t$, the $|[\Psi]|$ leads to a $6^{th}$-order polynomial. The roots of this polynomial represent the force-unconstrained poses of the manipulator, where $\phi$ is obtained from $t$, and $x$ and $y$ are found from the first two rows of Eq. (6), i.e.,

$$\begin{bmatrix} x \\ y \end{bmatrix} = - \begin{bmatrix} \psi_{11} & \psi_{12} \\ \psi_{21} & \psi_{22} \end{bmatrix}^{-1} \begin{bmatrix} \psi_{13} \\ \psi_{23} \end{bmatrix} \tag{7}$$

Given that there are eight possible solutions of the inverse kinematics [19], an identification of the solutions that lead to singular configurations is carried out. One pose may make two or more solutions of the inverse kinematics singular. That is, the singular configurations of each solution of the inverse kinematics is described by a surface in the $x - y - \phi$ space and whenever these surfaces intersect two or more solutions of the inverse kinematics are singular.

The obtained position of the platform is referred to the origin of *{ref}*. However, it can be transformed to a frame *{cen}* located at the centre of the platform and oriented as *{ref}*.

***Example.-***A numerical example of the force-unconstrained poses of the centre of the platform of the 3-PRR manipulator is presented. The bases are arranged in a triangular form 500 $mm$ apart, the angle of the bases are $\gamma_1 = -90°$, $\gamma_2 = 30°$, and $\gamma_3 = 150°$, $\rho_i = l_2 = l_3 = 200\ mm$, for $i$ = 1,2,3, and $\alpha_3 = 60°$. Figure 2 illustrates, for each solution of the inverse kinematics[3], a surface of force-unconstrained poses in the $x - y - \phi$ space. The last plot shows the combination of all eight surfaces. Each plot shows their respective projections on the $xy$ plane.

[2] Half angle substitution is defined as $\sin(\phi) = 2t/(1+t^2)$ and $\cos(\phi) = (1-t^2)/(1+t^2)$, where $t = \tan(\phi/2)$.

[3] There are up to two solutions for each branch. Each configuration is labeled depending on the length of the prismatic joint + for longer and - for shorter.

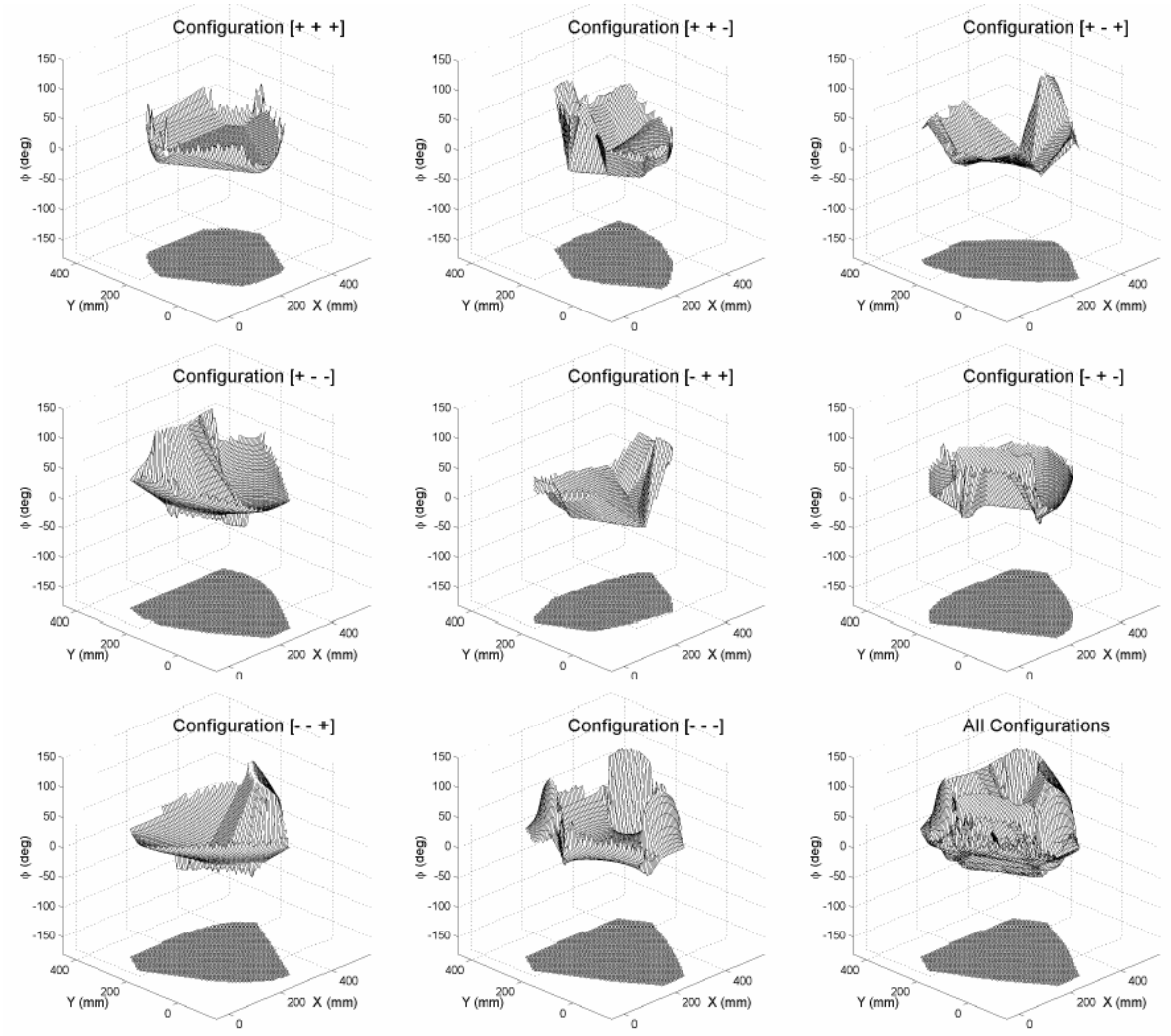


Figure 2: Force-Unconstrained poses of the 3-PRR manipulator

# 3 4-PRR Manipulator

## 3.1 Background

The inclusion of an additional actuated branch is based on having every branch actuated by a single actuator. For manipulators with redundant actuation, the ARS matrix is an $m \times n$ non-square matrix[4] and thus taking its determinant is not possible. A solution is to find conditions that make the determinant of all unique $m \times m$ ($3 \times 3$ for PPMs) sub-matrices equal to zero. This methodology was also mentioned in [8] and described in [13] as the intersection of the hypersurfaces in the $m-$dimensional task space forming a lower dimensional manifold. There are $\lambda = n!/(m!\,(n-m)!)$ unique combinations of sub-matrices, i.e., $|^{\text{ref}}[\mathbf{W}_j]| = 0$, for $j = 1, 2, ..., \lambda$. With one degree of redundancy, four sub-matrices exist, yielding four determinants. Nonetheless, two of these determinants are linearly dependent on the other two; therefore, only two combinations of non-redundant mechanisms have to be considered. In general, for every degree of redundancy one equation, beyond the one from the original non-redundant manipulator, is not linearly dependent.

[4] with $m < n$, where $m$ and $n$ are referred to the number of degrees of freedom and actuated joints, respectively.

The number of equations that are required to identify the force-unconstrained configurations of PPMs with redundant branches is the number of not linearly dependent determinants of the sub-matrices plus the number of branches. In particular for the 4-PRR manipulator, two not linearly dependent determinants and four branches lead to six equations in seven variables. In the following subsections, the required equations are derived and then through an elimination technique the singular configurations of the 4-PRR PPM are identified.

### 3.2 Derivation of Equations

The ARS of the redundant branch is

$$^{\text{ref}}W_{1_4} = \{-\cos(\theta_{3_4} - \alpha_4),\ \sin(\theta_{3_4} - \alpha_4); l_4 \sin\theta_{3_4}\}^T \tag{8}$$

Let the non-redundant mechanisms be composed of branches 1-2-3 and 1-2-4. The ARS matrices are assembled and their respective determinants are shown below:

$$\begin{aligned} \text{For branches 1-2-3,} \quad |^{\text{ref}}[\mathbf{W}_1]| &= l_2 \sin(\theta_{3_2})(\sin(\theta_{3_1})\cos(\theta_{3_3} - \alpha_3) - \cos(\theta_{3_1})\sin(\theta_{3_3} - \alpha_3)) \\ &\quad + l_3 \sin(\theta_{3_3})(\cos(\theta_{3_1})\sin(\theta_{3_2}) - \sin(\theta_{3_1})\cos(\theta_{3_2})) = 0 \end{aligned} \tag{9}$$

$$\begin{aligned} \text{For branches 1-2-4,} \quad |^{\text{ref}}[\mathbf{W}_2]| &= l_2 \sin(\theta_{3_2})(\sin(\theta_{3_1})\cos(\theta_{3_4} - \alpha_4) - \cos(\theta_{3_1})\sin(\theta_{3_4} - \alpha_4)) \\ &\quad + l_4 \sin(\theta_{3_4})(\cos(\theta_{3_1})\sin(\theta_{3_2}) - \sin(\theta_{3_1})\cos(\theta_{3_2})) = 0 \end{aligned} \tag{10}$$

The general loop-closure equation found in Eq. (5) is also applicable for the fourth branch.

### 3.3 Force-Unconstrained Poses

The force-unconstrained poses of the 4-PRR are defined as the intersection among the surfaces of two non-redundant 3-PRR PPMs. Since, the singular poses of each 3-PRR PPM are represented by a $20^{th}$-order polynomial [7], the force-unconstrained poses of the 4-PRR would be a $400^{th}$-order polynomial. This prediction is based on the Bezout number, which states that the total degree of a polynomial system is defined as the product of the degrees of all the polynomials [25].

There are six equations ($|^{\text{ref}}[\mathbf{W}_j]| = 0$ and $f_i(x, y, \phi, \theta_{3_i}) = 0$, $j = 1, 2$ and $i = 1, 2, 3, 4$) and seven variables ($x$, $y$, $\phi$, and $\theta_{3_i}$, $i = 1, 2, 3, 4$), i.e., there is one "free" variable. Let $\theta_{3_1}$ be the "free" variable and constant. Thus, a problem of six non-linear equations in six unknowns results,

$$\begin{aligned} f_1(x, y, \phi) &= 0 \quad \text{Loop-Closure Equation of branch 1} \\ f_2(x, y, \phi, \theta_{3_2}) &= 0 \quad \text{Loop-Closure Equation of branch 2} \\ f_3(x, y, \phi, \theta_{3_3}) &= 0 \quad \text{Loop-Closure Equation of branch 3} \\ f_4(x, y, \phi, \theta_{3_4}) &= 0 \quad \text{Loop-Closure Equation of branch 4} \\ g_1(\theta_{3_2}, \theta_{3_3}) &= 0 \quad \text{Determinant of submatrix composed by branches 1-2-3} \\ g_2(\theta_{3_2}, \theta_{3_4}) &= 0 \quad \text{Determinant of submatrix composed by branches 1-2-4} \end{aligned}$$

The solution of this problem requires an elimination technique, which is described as follows:

***Step 1***.- Apply half-angle substitution to the third joint angles, i.e., $\sin(\theta_{3_i}) = 2q_i/\left(1 + q_i^2\right)$ and $\cos(\theta_{3_i}) = \left(1 - q_i^2\right)/\left(1 + q_i^2\right)$, where $q_i = \tan(\theta_{3_i}/2)$. The new variables are substituted back in their respective equations and the denominators are cleared. For further convenience, the coefficients of the five power products of equations $g_1(q_2, q_3) = 0$ and $g_2(q_2, q_4) = 0$ are collected ($a_{jk}$ for $j = 1, 2$ and $k = 1, .., 5$) and shown in Appendix I.

$$g_1(q_2,\ q_3) = a_{11}q_3q_2^2 + a_{12}q_3^2q_2 + a_{13}q_3q_2 + a_{14}q_3 + a_{15}q_2 = 0 \tag{11}$$

$$g_2(q_2,\ q_4) = a_{21}q_4q_2^2 + a_{22}q_4^2q_2 + a_{23}q_4q_2 + a_{24}q_4 + a_{25}q_2 = 0 \tag{12}$$

***Step 2***.- Eliminate variable $x$ by isolating it from equation $f_1(x,\ y,\ \phi) = 0$ and substituting it back in equations $f_2(x,\ y,\ \phi,\ q_2) = 0$, $f_3(x,\ y,\ \phi,\ q_3) = 0$, and $f_4(x,\ y,\ \phi,\ q_4) = 0$. The new equations, $f_i'(y,\ \phi,\ q_i) = 0$ for $i = 2, 3, 4$, are composed of 10 power products. The coefficients of the power products are collected ($b_{ik}$ for $i = 2, 3, 4$ and $k = 1, .., 10$) and shown in Appendix I.

$$\begin{aligned} f_i'(y, \phi, q_i) &= b_{i1}q_i^2 y + b_{i2}q_i^2\cos(\phi) + b_{i3}q_i^2\sin(\phi) + b_{i4}q_i^2 + b_{i5}q_i\cos(\phi) \\ &\quad + b_{i6}q_i\sin(\phi) + b_{i7}\cos(\phi) + b_{i8}\sin(\phi) + b_{i9}y + b_{i10} \end{aligned} \tag{13}$$

***Step 3***.- Eliminate variable $y$ by isolating it from equation $f_2'(y,\ \phi,\ q_2) = 0$ and substituting it back in equations $f_3'(y,\ \phi,\ q_3) = 0$, and $f_4'(y,\ \phi,\ q_4) = 0$. The new equations, $f_i''(\phi,\ q_2,\ q_i) = 0$ for $i = 3, 4$, are composed of 20 power products. The coefficients of the power products are collected ($c_{ik}$ for $i = 3, 4$ and $k = 1, .., 20$) and shown in Appendix I.

$$\begin{aligned} f_i''(\phi,\ q_2,\ q_i) &= c_{i1}q_2^2q_i^2\cos(\phi) + c_{i2}q_2^2q_i^2\sin(\phi) + c_{i3}q_2^2q_i\cos(\phi) + c_{i4}q_2^2q_i\sin(\phi) + c_{i5}q_2^2\cos(\phi) \\ &\quad + c_{i6}q_2^2\sin(\phi) + c_{i7}q_2^2q_i^2 + c_{i8}q_2^2 + c_{i9}q_2q_i^2\cos(\phi) + c_{i10}q_2q_i^2\sin(\phi) \\ &\quad + c_{i11}q_2\cos(\phi) + c_{i12}q_2\sin(\phi) + c_{i13}q_i^2\cos(\phi) + c_{i14}q_i^2\sin(\phi) + c_{i15}q_i\cos(\phi) \\ &\quad + c_{i16}q_i\sin(\phi) + c_{i17}\cos(\phi) + c_{i18}\sin(\phi) + c_{i19}q_i^2 + c_{i20} \end{aligned} \tag{14}$$

***Step 4***.- Eliminate variable $q_3$ by isolating it from equation $g_1(q_2,\ q_3) = 0$ and substituting it back in equation $f_3''(\phi,\ q_2,\ q_3) = 0$. Similarly, eliminate variable $q_4$ by isolating it from equation $g_2(q_2,\ q_4) = 0$ and substituting it back in equation $f_4''(\phi,\ q_2,\ q_4) = 0$. These two eliminations are not as simple as the previous ones because the variables being eliminated are non-linear. In order to get rid of the square roots that appear after the substitutions, the expressions have to be squared. This leads to two new equations $h_j(\phi,\ q_2) = 0$, for $j = 1, 2$.

***Step 5***.- Apply half-angle substitution to $\phi$. Let $t$ be the corresponding variable after the substitution, yielding $h_j(t,\ q_2) = 0$, for $j = 1, 2$. These two expressions contain 45 power products because $q_2$ is a variable of degree 8 and $t$ is a variable of degree 4. The power products are grouped and the coefficients $d_{jr}$, where $r = 5i + k + 1$, are collected.

$$h_j(t, q_2) = \sum_{i=0}^{8}\sum_{k=0}^{4} d_{jr}\, q_2^i\, t^{\,k} = 0 \tag{15}$$

***Step 6***.- Assemble a 2 by 5 matrix $[\Psi']$ by sorting the powers of $t$. This matrix is generated with equations $h_1(t,\ q_2) = 0$ and $h_2(t,\ q_2) = 0$, and its entries are $8^{th}$-order polynomials in $q_2$.

$$\left[\Psi'\right]\ \mathbf{t}' = \mathbf{0} \tag{16}$$

where $[\Psi'] = \begin{bmatrix} \psi_{11} & \psi_{12} & \psi_{13} & \psi_{14} & \psi_{15} \\ \psi_{21} & \psi_{22} & \psi_{23} & \psi_{24} & \psi_{25} \end{bmatrix}$ and $\mathbf{t}' = \begin{bmatrix} t^4 & t^3 & t^2 & t & 1 \end{bmatrix}^{\mathrm{T}}$.

***Step 7***.- Generate additional equations, such that the number of equations matches the number of power products. Equations $h_1(t,\ q_2) = 0$ and $h_2(t,\ q_2) = 0$ are multiplied by $t$, $t^2$, and $t^3$. This leads to an 8 by 8 matrix, whose entries are still $8^{th}$-order polynomials in $q_2$.

$$[\Psi]\ \mathbf{t} = \begin{bmatrix} \psi_{11} & \psi_{12} & \psi_{13} & \psi_{14} & \psi_{15} & 0 & 0 & 0 \\ \psi_{21} & \psi_{22} & \psi_{23} & \psi_{24} & \psi_{25} & 0 & 0 & 0 \\ 0 & \psi_{11} & \psi_{12} & \psi_{13} & \psi_{14} & \psi_{15} & 0 & 0 \\ 0 & \psi_{21} & \psi_{22} & \psi_{23} & \psi_{24} & \psi_{25} & 0 & 0 \\ 0 & 0 & \psi_{11} & \psi_{12} & \psi_{13} & \psi_{14} & \psi_{15} & 0 \\ 0 & 0 & \psi_{21} & \psi_{22} & \psi_{23} & \psi_{24} & \psi_{25} & 0 \\ 0 & 0 & 0 & \psi_{11} & \psi_{12} & \psi_{13} & \psi_{14} & \psi_{15} \\ 0 & 0 & 0 & \psi_{21} & \psi_{22} & \psi_{23} & \psi_{24} & \psi_{25} \end{bmatrix} \begin{bmatrix} t^7 \\ t^6 \\ t^5 \\ t^4 \\ t^3 \\ t^2 \\ t \\ 1 \end{bmatrix} = \mathbf{0} \tag{17}$$

***Step 8***.- Eliminate variable $t$ by making matrix $[\Psi]$ singular, i.e., making Eq. (17) valid. Solving $|[\Psi]| = 0$ is complicated, because each entry of $[\Psi]$ is an $8^{th}$-order polynomial. The resulting determinant will be a $64^{th}$-order polynomial. Therefore, the computation of the roots of such a large polynomial may be susceptible to having floating point arithmetic problems. As an alternative, the roots of $|[\Psi]| = 0$ can be found as a generalized eigenvalue problem [26]. Matrix $[\Psi]$ can be written as a matrix polynomial; i.e.,

$$[\Psi] = \sum_{i=0}^{8} [\Psi_i]\, q_2^i \tag{18}$$

where each entry of $[\Psi_i]$ corresponds to one of the coefficients $d_{jr}$ as in Eq. (15).

The idea of this method is to assemble a 64 by 64 matrix $[\mathbf{K}]$ with each matrix $[\Psi_i]$ of Eq. (18).

$$[\mathbf{K}] = \begin{bmatrix} \mathbf{0} & \mathbf{I} & \cdots & \mathbf{0} \\ \vdots & \vdots & \ddots & \vdots \\ \mathbf{0} & \mathbf{0} & \cdots & \mathbf{I} \\ -[\Psi_8]^{-1}[\Psi_0] & -[\Psi_8]^{-1}[\Psi_1] & \cdots & -[\Psi_8]^{-1}[\Psi_7] \end{bmatrix} \tag{19}$$

where $\mathbf{0}$ and $\mathbf{I}$ are 8 by 8 null and identity matrices, respectively.

The eigenvalues of matrix $[\mathbf{K}]$ correspond precisely to the roots of the sixty-forth order polynomial, i.e., all solutions of $q_2$ for a given value of $\theta_{3_1}$.

***Step 9***.- Compute the poses of the manipulator by back substituting the numerical values of $q_2$. Variable $t$ can be determined by inverting the first seven rows and columns of matrix $[\Psi]$ and multiplying the minus of the first seven elements of the last column of $[\Psi]$, similar to Eq. (7).

The already known variables can be transformed to their original angle expressions by using the half-angle substitution property, i.e., $t \Longrightarrow \phi$ and $q_2 \Longrightarrow \theta_{3_2}$. Finally, equations $f_1(x, y, \phi) = 0$ and $f_2(x, y, \phi, \theta_{3_2}) = 0$ lead to a system of linear equations, where $x$ and $y$ can be found.

***Example.-***The singular poses of a 4-PRR with the following characteristics is presented, the bases are arranged in a square form 2 $m$ apart, the angle of the bases are $\gamma_1 = 0°$, $\gamma_2 = 90°$, $\gamma_3 = 180°$, and $\gamma_4 = 270°$, $\rho_i = l_2 = l_4 = 1$ $m$, for $i$ = 1,2,3,4, $l_3 = 2/\sqrt{2}$ $m$, $\alpha_3 = 45°$, and $\alpha_4 = 90°$. Figure 3a illustrates the loci of the single order of force-unconstrained poses of the platform centre in the $x - y - \phi$ space. Figure 3b is a projection of the curves on the $xy$ plane.

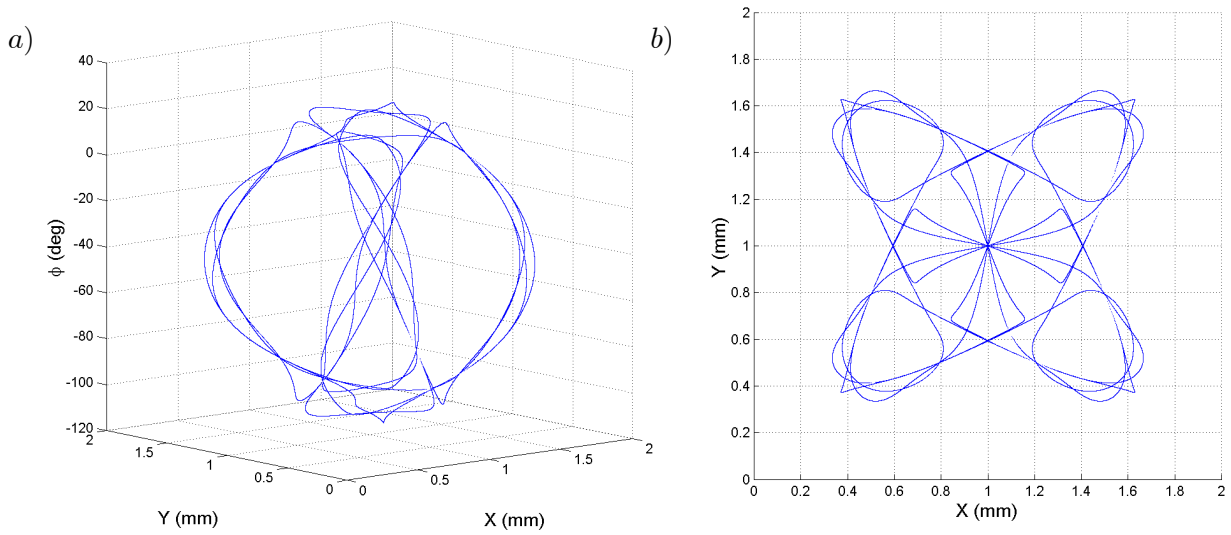


Figure 3: Force-Unconstrained poses of the 4-PRR manipulator

## 4 Discussion

The importance of referring the ARS wrt an inertial reference frame allows us to find concise expressions of the conditions that cause PPMs to be in singular configurations. It is important to mention that the lengths of the links and the distance between bases must be scaled before solving these problems numerically. Large numbers may cause floating point arithmetic errors.

The method used to find the roots of a sixty-forth order polynomial of the 4-PRR, the generalized eigenvalue problem, reduces considerably computation time and makes the problem much more stable. However, it is prone to having erroneous solutions due to defective eigenvalues. That is, the problem of computing multiple roots can be ill-conditioned. In many cases the solution has a multiplicity greater than one; in general, these eigenvalues come out as two identical real numbers (multiplicity of two) but do not correspond to any solution of the problem.

## 5 Conclusion

In this research, two major achievements have been accomplished. First, an efficient solution for identifying all singular configurations of the 3-PRR PPM was presented. In the literature, the force-unconstrained poses of this manipulator are mathematically represented by a twentieth order polynomial. In this paper, such configurations are obtained by selecting appropriate "free" variables. A sixth order polynomial related to force-unconstrained configurations, providing better computation efficiency, results. Second, a method to obtain all singular configurations of the 4-PRR, a redundant PPM with an additional actuated branch, was presented. Despite the mathematical difficulty of this problem, due to the non-linearity of the equations, a very effective elimination technique was adopted. In both cases, the solutions were found symbolically allowing implementation to any similar manipulator.

## Acknowledgements

The authors wish to thank the Natural Sciences and Engineering Research Council (NSERC) of Canada for providing financial support for this research.

## References

[1] J. P. Merlet, "Singular configurations of parallel manipulators and Grassmann geometry," *Int J Robot Res*, 8:(5), 45-56, 1989.

[2] C. M. Gosselin and J. Angeles, "Singularity analysis of closed-loop kinematic chains," *IEEE Trans Rob Autom*, 6:(3), 281-290, 1990.

[3] J. Sefrioui and C. M. Gosselin, "On the quadratic nature of the singularity curves of planar three-degree-of-freedom parallel manipulators," *Mech Mach Theory*, 30:(4), 533-551, 1995.

[4] I. A. Bonev and C. M. Gosselin, "Singularity Loci of Planar Parallel Manipulators with Revolute Joints," in *Computational Kinematics*, (F.C. Park C.C. Iurascu eds.), 291-299, 2001.

[5] V. K. Chan and I. Ebert-Uphoff, "Investigation of the deficiencies of parallel manipulators in singular configurations through the Jacobian nullspace," in *IEEE Int Conf Robot Autom*, (Seoul, Korea), 1313-1320, 2001.

[6] I. A. Bonev, *Geometric Analysis of Parallel Mechanisms*. Ph.D. Dissertation, Laval University, Dep Mech Eng, QC, November 2002.

[7] I. A. Bonev, D. Zlatanov, and C. M. Gosselin, "Singularity analysis of 3-dof planar parallel mechanisms via screw theory," *J Mech Design*, 125:(3), 573-581, 2003.

[8] J. P. Merlet, "Redundant parallel manipulators," *J Lab Rob Autom*, vol. 8, 17-24, 1996.

[9] L. Notash and R. P. Podhorodeski, "Uncertainty configurations of three-branch manipulators: Identification and elimination," in *ASME 23rd Bien Mech Conf*, (Minneapolis, MN), 459-466, 1994.

[10] L. Notash and R. P. Podhorodeski, "Forward displacement analysis and uncertainty configurations of parallel manipulators with a redundant branch," *J Robot Syst*, 13:(9), 587-601, 1996.

[11] S. B. Nokleby, R. Fisher, R. P. Podhorodeski, and F. Firmani, "Force capabilities of redundantly-actuated parallel manipulators," *Mech Mach Theory*, 40:(5), 578-599, 2005.

[12] C. L. Collins, *Singularity Analysis and Design of Parallel Manipulators*. PhD Thesis, Mechanical and Aerospace Engineering, University of California, Irvine, 1997.

[13] B. Dasgupta and T. S. Mruthyunjaya, "Force redundancy in parallel manipulators: Theoretical and practical issues," *Mech Mach Theory*, 33:(6), 727-742, 1998.

[14] J. F. O'Brien and J. T. Wen, "Redundant actuation for improving kinematic manipulability," in *Proc IEEE Int Conf Robot Autom*, (Detroit, MI), 1520-1525, 1999.

[15] V. K. Chan, *Singularity Analysis and Redundant Actuation of Parallel Manipulators*. M.Sc. Thesis, Georgia Institute of Technology, March 2001.

[16] F. Firmani and R. P. Podhorodeski, "Force-unconstrained poses for a redundantly-actuated planar parallel manipulator," *Mech Mach Theory*, 39:(5), 459-476, 2004.

[17] F. Firmani and R. P. Podhorodeski, "Force degeneracies for a redundantly actuated planar parallel manipulator," in *Proc CSME Forum 2002*, (Kingston, ON), 9 pp., 2002.

[18] F. Firmani and R. P. Podhorodeski, "Force-unconstrained poses for parallel manipulators with redundant actuated branches," in *Proc CSME Forum 2004*, (London, ON), 9 pp., 2004.

[19] C. M. Gosselin, S. Lemieux, and J. P. Merlet, "A new architecture of planar three-degree-of-freedom parallel manipulator," in *IEEE Int Conf Robot Autom*, (Minneapolis, MN), 3738-3743, 1996.

[20] J. Denavit and R. S. Hartenberg, "A kinematic notation for lower-pair mechanisms based on matrices," *Trans ASME J Appl Mech*, 215-221, 1955.

[21] L. S. Woo and F. Freudenstein, "Application of line geometry to theoretical kinematics and the kinematic analysis of mechanical systems," *Trans ASME J Mech*, vol. 5, 417-460, 1970.

[22] K. Sugimoto, J. Duffy, and K. H. Hunt, "Special Configurations of Spatial Mechanisms and Robot Arms," *Mech Mach Theory*, 17:(2), 119-132, 1982.

[23] B. Roth, "Screws, motors, and wrenches that cannot be bought in a hardware store," *Robotics Research: The First International Symposium*, 679-693, 1984.

[24] K. H. Hunt, *Kinematic Geometry of Mechanisms*. Toronto: Oxford U.P., 1978.

[25] L. W. Tsai, *Robot Analysis, The Mechanics of Serial and Parallel Manipulators.* Toronto: Wiley-Interscience, 1999.

[26] H. G. Golub and C. F. Van Loan, *Matrix Computations.* Baltimore, MD: The Johns Hopkins University Press, 1983.

## Appendix I.- Coefficients of Power Products

Coefficients of power products in step 1:

$$[\mathbf{A}] = \begin{bmatrix} a_{1,1} & a_{1,2} & a_{1,3} & a_{1,4} & a_{1,5} \\ a_{2,1} & a_{2,2} & a_{2,3} & a_{2,4} & a_{2,5} \end{bmatrix}$$

$a_{i,1} = -2s_{3_1} l_j$
$a_{i,2} = 2c_{3_1} l_2 s\alpha_j + 2s_{3_1} l_2 c\alpha_j$
$a_{i,3} = -4c_{3_1} l_j + 4c_{3_1} l_2 c\alpha_j - 4s_{3_1} l_2 s\alpha_j$
$a_{i,4} = 2s_{3_1} l_j$
$a_{i,5} = -2c_{3_1} l_2 s\alpha_j - 2s_{3_1} l_2 c\alpha_j$

where $s_{3_1} = \sin(\theta_{3_1})$, $c_{3_1} = \cos(\theta_{3_1})$, $s\alpha_j = \sin(\alpha_j)$, and $c\alpha_j = \cos(\alpha_j)$, for $i = 1, 2$ and $j = 3, 4$.

Coefficients of power products in step 2:

$$[\mathbf{B}] = \begin{bmatrix} b_{1,1} & b_{1,2} & b_{1,3} & b_{1,4} & b_{1,5} & b_{1,6} & b_{1,7} & b_{1,8} & b_{1,9} & b_{1,10} \\ b_{2,1} & b_{2,2} & b_{2,3} & b_{2,4} & b_{2,5} & b_{2,6} & b_{2,7} & b_{2,8} & b_{2,9} & b_{2,10} \\ b_{3,1} & b_{3,2} & b_{3,3} & b_{3,4} & b_{3,5} & b_{3,6} & b_{3,7} & b_{3,8} & b_{3,9} & b_{3,10} \end{bmatrix}$$

$b_{i,1} = \sin(\gamma_j - \gamma_1)$
$b_{i,2} = \rho_1 \cos(\gamma_j) \sin(\gamma_1 - \alpha_1) s_{3_1} - (\rho_1 c_{3_1} + l_1) \cos(\gamma_j) \cos(\gamma_1 - \alpha_1) - (\rho_j - l_j) \cos(\gamma_1) \cos(\gamma_j - \alpha_j)$
$b_{i,3} = -\rho_1 \cos(\gamma_j) \cos(\gamma_1 - \alpha_1) s_{3_1} - (\rho_1 c_{3_1} + l_1) \cos(\gamma_j) \sin(\gamma_1 - \alpha_1) - (\rho_j - l_j) \cos(\gamma_1) \sin(\gamma_j - \alpha_j)$
$b_{i,4} = -\sin(\gamma_j) \cos(\gamma_1)\, by_j + \cos(\gamma_j) \sin(\gamma_1)\, by_1 - (bx_j - bx_1) \cos(\gamma_j) \cos(\gamma_1)$
$b_{i,5} = -2\rho_j \cos(\gamma_1) \sin(\gamma_j - \alpha_j)$
$b_{i,6} = 2\rho_j \cos(\gamma_1) \cos(\gamma_j - \alpha_j)$
$b_{i,7} = \rho_1 \cos(\gamma_j) \sin(\gamma_1 - \alpha_1) s_{3_1} - (\rho_1 c_{3_1} + l_1) \cos(\gamma_j) \cos(\gamma_1 - \alpha_1) + (\rho_j + l_j) \cos(\gamma_1) \cos(\gamma_j - \alpha_j)$
$b_{i,8} = -\rho_1 \cos(\gamma_j) \cos(\gamma_1 - \alpha_1) s_{3_1} - (\rho_1 c_{3_1} + l_1) \cos(\gamma_j) \sin(\gamma_1 - \alpha_1) + (\rho_j + l_j) \cos(\gamma_1) \sin(\gamma_j - \alpha_j)$
$b_{i,9} = \sin(\gamma_j - \gamma_1)$
$b_{i,10} = -\sin(\gamma_j) \cos(\gamma_1)\, by_j + \cos(\gamma_j) \sin(\gamma_1)\, by_1 - (bx_j - bx_1) \cos(\gamma_j) \cos(\gamma_1)$

for $i = 1, 2, 3$ and $j = i + 1$.

Coefficients of power products in step 3:

$$[\mathbf{C}] = \begin{bmatrix} c_{1,1} & c_{1,2} & \cdots & c_{1,19} & c_{1,20} \\ c_{2,1} & c_{2,2} & \cdots & c_{2,19} & c_{2,20} \end{bmatrix}$$

$c_{i,1} = -b_{j,1} b_{1,2} + b_{j,2} b_{1,1}$
$c_{i,2} = -b_{j,1} b_{1,3} + b_{j,3} b_{1,1}$
$c_{i,3} = b_{j,5} b_{1,1}$
$c_{i,4} = b_{j,6} b_{1,1}$
$c_{i,5} = b_{j,7} b_{1,1} - b_{j,9} b_{1,2}$
$c_{i,6} = -b_{j,9} b_{1,3} + b_{j,8} b_{1,1}$
$c_{i,7} = -b_{j,1} b_{1,4} + b_{j,4} b_{1,1}$
$c_{i,8} = b_{j,10} b_{1,1} - b_{j,9} b_{1,4}$
$c_{i,9} = -b_{j,1} b_{1,5}$
$c_{i,10} = -b_{j,1} b_{1,6}$
$c_{i,11} = -b_{j,9} b_{1,5}$
$c_{i,12} = -b_{j,9} b_{1,6}$
$c_{i,13} = -b_{j,1} b_{1,7} + b_{j,2} b_{1,9}$
$c_{i,14} = -b_{j,1} b_{1,8} + b_{j,3} b_{1,9}$
$c_{i,15} = b_{j,5} b_{1,9}$
$c_{i,16} = b_{j,6} b_{1,9}$
$c_{i,17} = b_{j,7} b_{1,9} - b_{j,9} b_{1,7}$
$c_{i,18} = -b_{j,9} b_{1,8} + b_{j,8} b_{1,9}$
$c_{i,19} = -b_{j,1} b_{1,10} + b_{j,4} b_{1,9}$
$c_{i,20} = b_{j,10} b_{1,9} - b_{j,9} b_{1,10}$

for $i = 1, 2$ and $j = i + 1$.